The severity of mammary gland developmental defects is linked to the overall functional status of Cx43 as revealed by genetically modified mice

Michael K. G. STEWART*, Xiang-Qun GONG*, Kevin J. BARR*, Donglin BAI*, Glenn I. FISHMAN† and Dale W. LAIRD*‡[1]

*Department of Physiology and Pharmacology, Western University, London, ON, Canada N6A 5C1, †Division of Cardiology, New York University School of Medicine, New York, NY 10016, U.S.A., and ‡Department of Anatomy and Cell Biology, Western University, London, ON, Canada N6A 5C1

Genetically modified mice mimicking ODDD (oculodentodigital dysplasia), a disease characterized by reduced Cx43 (connexin 43)-mediated gap junctional intercellular communication, represent an *in vivo* model to assess the role of Cx43 in mammary gland development and function. We previously reported that severely compromised Cx43 function delayed mammary gland development and impaired milk ejection in mice that harboured a G60S Cx43 mutant, yet there are no reports of lactation defects in ODDD patients. To address this further, we obtained a second mouse model of ODDD expressing an I130T Cx43 mutant to assess whether a mutant with partial gap junction channel activity would be sufficient to retain mammary gland development and function. The results of the present study show that virgin Cx43$^{I130T/+}$ mice exhibited a temporary delay in ductal elongation at 4 weeks. In addition, Cx43$^{I130T/+}$ mice develop smaller mammary glands at parturition due to reduced cell proliferation despite similar overall gland architecture. Distinct from Cx43$^{G60S/+}$ mice, Cx43$^{I130T/+}$ mice adequately produce and deliver milk to pups, suggesting that milk ejection is unaffected. Thus the present study suggests that a loss-of-function mutant of Cx43 with partial gap junction channel coupling conductance results in a less severe mammary gland phenotype, which may partially explain the lack of reported lactation defects associated with ODDD patients.

Key words: connexin 43, development, gap junctional intercellular communication, mammary gland, milk ejection, oculodentodigital dysplasia.

INTRODUCTION

ODDD (oculodentodigital dysplasia) is a rare pleiotropic disease characterized by developmental symptoms that include craniofacial defects, cornea and lens abnormalities, tooth defects and syndactyly of the digits [1]. This disease is linked to mainly autosomal dominant mutations in the *GJA1* gene which encodes Cx43 (connexin 43) [1]. Cx43 is one of 21 connexins found in humans and is characterized by its ability to form hexameric gap junction channels that allow for the passage of molecules less than 1 kDa in size between the intracellular environments of adjacent cells [2]. This process, known as GJIC (gap junctional intercellular communication), is critical for the maintenance of key cellular processes including proliferation, differentiation and apoptosis in almost all cell types found in the human body, including the mammary gland [2,3].

The mammary gland of mice is comparable with that of humans in that it consists of a converging branched epithelial ductal network embedded within a stromal mammary fat pad [4]. The epithelium of the mammary gland is very dynamic and undergoes two major phases of development, one during puberty and one following the onset of pregnancy [4]. At birth, a rudimentary ductal tree exists within the stroma of the mammary gland which begins significant branch elongation and amplification following the onset of hormones at puberty [5]. By 10 weeks, full extension of ducts throughout the fat pad is achieved and a series of branching and regression cycles begin in response to the oestrous cycle [6]. At the onset of pregnancy, alveogenesis occurs in which secretory alveolar cells develop to produce milk for the pups throughout lactation [4]. Following weaning of the pups, the mammary gland undergoes extensive

gland remodelling to revert back to a virgin gland state in a process known as involution [4]. Throughout these developmental changes, the gland requires exquisite regulation of proliferation, differentiation and apoptosis to allow for the proper growth and development of ducts throughout puberty, differentiation of secretory alveolar cells for milk production throughout pregnancy and extensive gland remodelling following cessation of lactation [4]. Although the hormonal regulation of these cell processes is well documented, less is known about locally acting factors such as gap junction proteins and intercellular communication [5,7].

The human mammary gland is known to express two connexins: Cx26 localized to the luminal cells of ducts and alveoli, and Cx43, which is mainly restricted to the surrounding contractile myoepithelial cells and stromal fibroblasts [8,9]. This expression is similar in mice, with the addition of Cx32 and Cx30 in luminal cells which are able to form heteromeric/heterotypic channels with Cx26 for additional luminal cell regulation that is not found in humans [10,11]. Cx26, Cx30 and Cx32 have all been detected at low levels at all stages of development and, importantly, are temporally up-regulated during pregnancy, lactation and/or involution, suggesting that these connexins may regulate gland differentiation and function during these stages of development [12,13]. In contrast, Cx43 is constitutively expressed throughout mammary gland development, suggesting that Cx43 may have an important role in the maintenance of myoepithelial differentiation and co-ordinating function [14]. In addition, the importance of myoepithelial cells in the regulation of luminal cells through the induction of luminal cell polarity and through paracrine factors during branching morphogenesis suggests that dysregulation of myoepithelial cells may affect whole-gland development and function [15,16].

Abbreviations used: Cx, connexin; DMEM, Dulbecco's modified Eagle's medium; GFP, green fluorescent protein; GJIC, gap junctional intercellular communication; ODDD, oculodentodigital dysplasia; PCNA, proliferating cell nuclear antigen; TEB, terminal end bud; WAP, whey acidic protein; WT, wild-type.

[1] To whom correspondence should be addressed (email dale.laird@schulich.uwo.ca).

Previously, to assess the role of Cx43 in mammary gland development and function, a mutant mouse model of ODDD ($Gja1^{Jrt/+}$ mice; also called Cx43$^{G60S/+}$ mice) was evaluated as these mice express a dominant-negative mutant of Cx43 that reduces total Cx43 protein levels by far greater than 50% [17]. Cx43$^{G60S/+}$ mice express classical symptoms of ODDD including craniofacial abnormalities, loss of tooth enamel and syndactyly of the digits [17,18], despite the fact that the glycine to serine substitution at position 60 of Cx43 has never been reported in ODDD patients [19]. Interestingly, severely decreased levels of Cx43 in virgin Cx43$^{G60S/+}$ mice resulted in impaired stromal development of the fat pad, smaller mammary glands and a delay in ductal development between 4 and 10 weeks, suggesting an important role for Cx43 in regulating gland maturation in virgin mice [20]. In addition, lactating Cx43$^{G60S/+}$ mice displayed impaired milk secretion and milk accumulation in the gland as a result of improper milk ejection [20,21]. As a result, it was suggested that ODDD patients may also present with a defect in their ability to breast feed. However, despite over 65 identified mutations in *GJA1* resulting in ODDD, there have been no reports of lactation defects in humans with this rare disease [19]. Importantly, at least a population of females with ODDD are fertile and there have been reports of mothers with ODDD in multi-generational families [22].

Functional characterization of electrical gap junction coupling in model cell systems that express only ODDD-linked mutants revealed two distinct populations of mutants that form gap junctions: mutants that have residual channel activity (such as the human mutants K134E, L90V and I130T) and mutants that are functionally dead (such as the human G21R, Y17S and A40V, and mouse G60S mutants) [23,24]. It is unknown whether the severe mammary gland phenotype observed in Cx43$^{G60S/+}$ mice is indicative of patients expressing ODDD mutants lacking residual channel function or whether a Cx43 mutant with residual channel function would rescue the functional and developmental defects in the mammary gland observed in Cx43$^{G60S/+}$ mice. To investigate this, we obtained a mouse model of ODDD (Cx43$^{I130T/+}$) expressing an I130T autosomal-dominant mutant of Cx43 which is known to be expressed within the human population and maintains a junctional conductance of approximately 50% when co-expressed with WT (wild-type) Cx43 in the heart [25]. We hypothesized that these mutant mice would have fewer mammary gland defects as a result of a less severe reduction in Cx43-based levels of GJIC. Consequently, if this hypothesis was supported, it may help to explain why female patients with ODDD do not typically present with breast-feeding problems.

MATERIALS AND METHODS

Constructs

The construct encoding the Cx43 G60S mutant has been described previously [17]. The I130T–GFP (green fluorescent protein) cDNA construct was generated using the QuikChange® site-directed mutagenesis kit (Stratagene) using the Cx43–GFP construct as a template and the primers 5′-CACTTGAAGCAG-ACTGAGATAAAGAAG-3′ (forward) and 5′-CTTCTTTATC-TCAGTCTGCTTCAAGTG-3′ (reverse). The I130T mutant was verified by sequencing.

Patch-clamp electrophysiology

N2A (neuroblastoma) cells were transfected with GFP-tagged WT and mutant Cx43 respectively. At 24 h later, the isolated cell pairs with green fluorescence were selected to assess the intercellular coupling with dual whole-cell patch-clamp recordings. Both cells were initially held at the same voltage potential (0 mV), an impulse of −20 mV was then applied to one cell and the junctional current was recorded from the other cell. Gap junctional conductance (Gj) was calculated and presented as the mean ± S.E.M. Online series resistance compensation at 80% or off-line series resistance compensation were applied to improve the accuracy of the measured Gj [26].

Animals

Heterozygote mice expressing the I130T mutant were created as described by Fishman and colleagues [25] and were bred on a mixed background of CD1 and C57BL/6 ($Gja1^{tm3GFi}$) mice. All Cx43$^{I130T/+}$ mice used were at generation 1–4 of backcrossing to C57BL/6 and compared with WT littermate controls. Both virgin and pregnant female mice at various ages were killed using CO_2. Inguinal mammary glands were used for weight measurement, whole mounts and paraffin embedding. Thoracic mammary glands were collected for Western blot analysis and were stored at −80°C. Lactating mice were collected at day 21 of lactation. Pups from dams were weaned on day 21 of lactation and mammary glands from dams were collected 48 h post-weaning, which we denote as the involution time point. Lactating mice killed for the oxytocin-induced milk ejection assay were used no more than 3 days following parturition. Blood was collected via cardiac puncture from pregnancy day 9.5 mutant and WT mice. In addition, heterozygote $Gja1^{Jrt/+}$ ($Gja1^{m1Jrt}$; also known as Cx43$^{G60S/+}$) mice carrying the G60S mutant on a background of C3H/HeJ and C57BL/6J mice were used for primary culture experiments. Cx43$^{G60S/+}$ mice used in the experiments were compared with littermate and non-littermate controls. All experiments were approved by the Animal Care Committee at Western University and conducted according to the guidelines of the Canadian Council on Animal Care. For all experiments, $n = 6$ unless otherwise specified.

Primary cultures

Myoepithelial cells

Primary myoepithelial cells were isolated from adult Cx43$^{I130T/+}$ mice, Cx43$^{G60S/+}$ mice and their respective controls, similar to that described in Plante and Laird [27]. Dissected inguinal and thoracic mammary glands were minced and digested in 12 ml of collagenase solution [0.2% trypsin, 0.2% collagenase A, 5% fetal bovine serum and 5 μg/ml gentamycin in DMEM (Dulbecco's modified Eagle's medium)/F12] at 37°C for 30 min with gentle shaking (200 rev./min). The cell suspension was centrifuged for 10 min at 500 g and both the supernatant (containing undigested tissue in the fat pad) and the pellet were pipetted up and down to further separate epithelial organoids from adipocytes and both were re-centrifuged as before. Pellets from both the first and second centrifugation steps were combined into 4 ml of serum-free DMEM/F12 and 40 μl of DNase (2 units/ml) was added to the cell suspension. Cell suspensions were shaken by hand for 5 min at room temperature (21°C) prior to the addition of 6 ml of serum-free DMEM/F12 and centrifugation at 500 g for 10 min. The supernatant was discarded and the pellet was resuspended in 10 ml of serum-free DMEM/F12. The cell suspension was briefly centrifuged for 10 s and the supernatant was discarded. The pellet was then resuspended in serum-free DMEM/F12 and this centrifugation process was repeated six times to remove fibroblasts. The final cell pellet was resuspended

in 150 μl of MEGM (mammary epithelial cell growth medium) and plated directly on to a coverslip. All pipettes and tubes used during the procedure were pre-coated with sterile PBS containing 5% BSA. Myoepithelial cells were grown for 1 week before microinjection ($n = 3$).

Granulosa cells

Ovaries from adult Cx43$^{I130T/+}$ and Cx43$^{G60S/+}$ mice and their respective controls were digested in a collagenase and DNase solution [2 mg/ml type I collagenase (Sigma) and 0.02% DNase I (Sigma) in complete Waymouth Medium MB 752/1 (Sigma)] at 37°C. Follicles were isolated through repeated aspiration and expulsion with a 1-ml pipette. Follicles were washed twice and transferred to another dish in which the oocytes were separated from the granulosa cells by treatment with 0.05% trypsin-EDTA for 10 min followed by repeated pipetting and centrifugation at 600 g for 5 min. The supernatant was removed and granulosa cells were washed with Waymouth medium once and a second time in M199 medium containing Earle's salts and glutamine (Life Technologies). Granulosa cells were resuspended in M199 medium and cultured on 12-mm glass coverslips coated with collagen and incubated at 37°C in 5% CO_2/95% air.

Microinjection

For microinjection experiments, one cell within patches of confluent myoepithelial or granulosa cells was microinjected with 0.5% Lucifer Yellow (Molecular Probes) using an Eppendorf Femtojet automated pressure microinjector. Images were collected using a Leica DM IRE2 inverted epifluorescence microscope and the percentage of cells that passed dye to at least one neighbour as well as the number of cells that received the dye after 1 min and the average number of cells receiving dye after 1 min was recorded. Cells from three independent cell cultures from different mouse preparations were each injected 10–15 times for a total of $\sim$43–50 injections per mouse model.

Western blot analysis

Mammary gland tissue was homogenized using a tissue homogenizer in a lysis buffer [1% Triton X-100, 150 mM NaCl, 10 mM Tris/HCl (pH 7.4), 1 mM EDTA, 1 mM EDTA and 0.5% Nonidet P40, supplemented with protease inhibitor mixture (Roche Applied Sciences) and phosphatase inhibitors (100 mM sodium fluoride and 100 mM sodium orthovanadate)]. Protein lysate concentrations were measured using a BCA (bicinchoninic acid) protein determination kit (Pierce). Total protein lysates (60 μg) were resolved by SDS/PAGE (10% or 15% gels) and transferred on to nitrocellulose membranes using the iBlot Dry Blotting System (Invitrogen). Membranes were blocked using 3% BSA (Sigma) for 1 h before being immunolabelled with the primary antibodies rabbit anti-Cx43 (1:5000 dilution, Sigma), goat anti-β-casein (1:1000 dilution, Santa Cruz Biotechnology) and goat anti-WAP (whey acidic protein) (1:1000 dilution, Santa Cruz Biotechnology) and mouse anti-β-actin (1:200 dilution, Santa Cruz Biotechnology) at 4°C. Primary antibodies were detected using the fluorescently conjugated secondary antibodies anti-mouse IRdye 800 (1:5000 dilution, LI-COR Biosciences) and anti-rabbit IRdye 680 (1:5000 dilution, LI-COR Biosciences), scanned and quantified using the Odyssey Infrared Imaging System (LI-COR Biosciences).
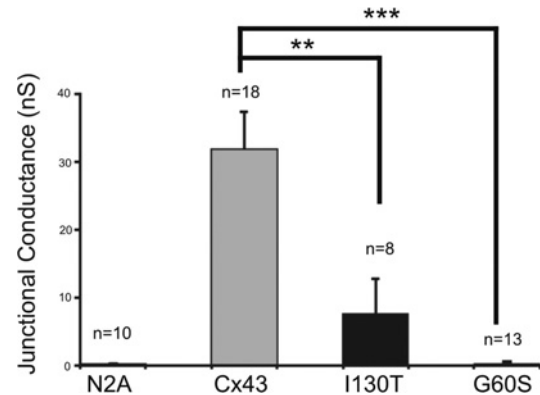
Figure 1   The Cx43 I130T mutant has reduced gap junctional coupling conductance

Junctional conductance measurements of gap junctional intercellular communication-deficient control N2A cells engineered to express Cx43 or the G60S or I130T mutants. The I130T mutant had reduced channel conductance (Gj) compared with WT Cx43, whereas the G60S mutant channels were completely non-functional. Values are mean levels of electrical conductance $\pm$ S.E.M. **$P < 0.01$; ***$P < 0.001$.

Immunofluorescence and microscopy

Paraffin-embedded sections (6 μm) were deparaffinized in xylene, rehydrated in descending concentrations of ethanol baths (100, 95, 70 and 50%) and, subsequently, microwaved for 5 min in antigen-retrieval solution (1:50, Vector Labs). After cooling for 20 min, slides underwent a second antigen retrieval using 0.01 M Tris/1 mM EDTA buffer (pH 9.0) at 90–95°C for 30 min, followed by another cooling for 20 min. Cryosections (6 μm) were fixed in neutral-buffered formalin for 15 min before blocking. Slides were blocked in 3% BSA/0.1% Triton X-100 in PBS for 60 min. Slides were probed with the primary antibodies rabbit anti-Cx43 antibody (1:500 dilution, Sigma), rabbit anti-Cx30 (1:100 dilution, Invitrogen), rabbit anti-Cx26 (1:100 dilution, Invitrogen), rabbit anti-Cx32 (1:100 dilution, Sigma), mouse anti-keratin14 (1:100 dilution, Neomarkers), mouse anti-PCNA (proliferating cell nuclear antigen) clone PC10 (1:200 dilution, Dako) or rabbit anti-(cleaved caspase 3) (1:400 dilution, Cell Signaling Technology) for 1 h at 37°C, followed by Alexa Fluor® 555-conjugated anti-rabbit (1:400 dilution, Molecular Probes) and Alexa Fluor® 633-conjugated anti-mouse (1:400 dilution, Molecular Probes) secondary antibodies. Nuclei were labelled with Hoechst 33342. Slides were mounted using Airvol. Images were captured using a Leica DM IRE2 inverted epifluorescence microscope and Openlab 5.5.3 imaging software. For quantification, eight to ten arbitrary images were taken at 20$\times$ magnification for each sample and the numbers of positive cells or plaques were counted relative to the area of nuclear staining that was measured using ImageJ 1.46r (NIH).

Evaluation of serum prolactin concentration

Four mutant and WT littermate mice were mated and killed at day 9.5 of pregnancy. Blood was collected via cardiac puncture and allowed to clot overnight at 4°C. Samples were centrifuged at 2000 g for 5 min and serum was collected and stored at -80°C. Prolactin concentrations were assessed by a prolactin mouse ELISA Kit (Abcam).

Whole mounting

Inguinal mammary glands were excised and processed as described previously [28]. Briefly, mammary glands were
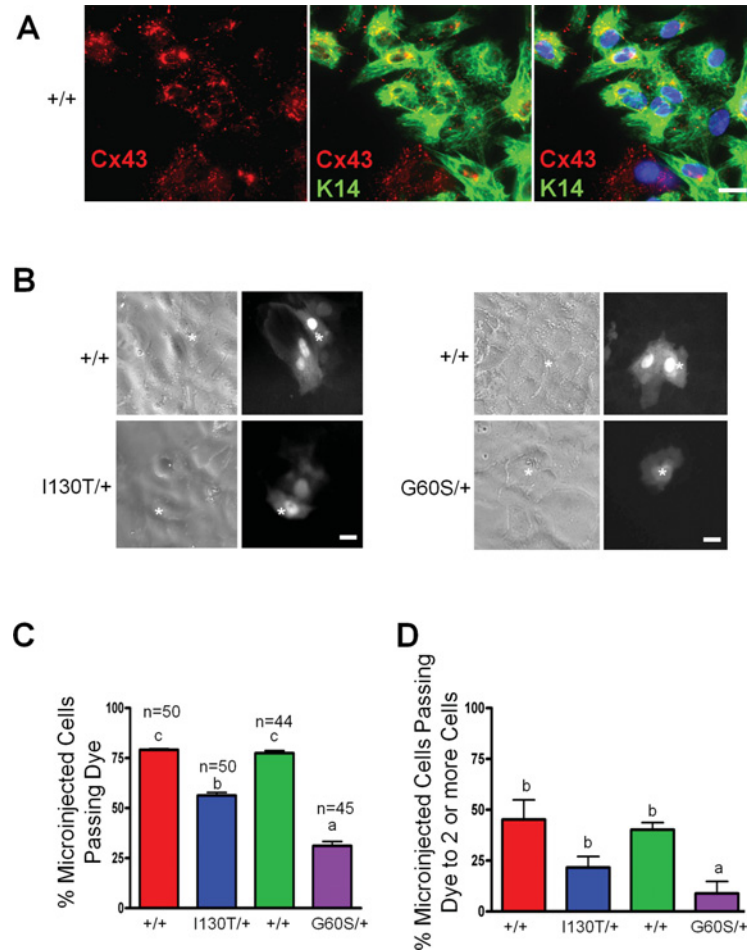
Figure 2   Myoepithelial cells isolated from Cx43^I130T/+ and Cx43^G60S/+ exhibit differential gap junction coupling relative to their respective controls

(**A**) Representative isolation of primary mammary epithelial cells from control mice are highly enriched for myoepithelial cells that form gap junctions based on keratin 14 (K14) (green) and Cx43 (red) labelling respectively. (**B**) Clusters of myoepithelial cells from Cx43^I130T/+ mice, Cx43^G60S/+ mice and their respective controls, were microinjected with Lucifer Yellow dye (asterisks). Scale bars = 10 μm. (**C**) Relative to controls, dye coupling was greater in cells expressing the I130T mutant than the G60S mutant. (**D**) Dye transfer to two or more cells was significantly reduced in myoepithelial cells from Cx43^G60S/+ mice only. Values are the mean percentage incidence of dye transfer $\pm$ S.E.M. from three experiments. In (**C**), *n* indicates the number of injections. Letters on top of columns in (**C**) and (**D**) represent statistical differences.

spread on a glass slide and fixed in Carnoy's fixative (100 % ethanol/chloroform/glacial acetic acid; 6:3:1, by vol.) overnight at 4 °C. Mammary glands were washed in 70 % ethanol for 15 min and gradually rehydrated in water. Glands were stained overnight in carmine alum (2 % carmine and 5 % aluminium potassium sulfate in water) at room temperature. Mammary glands were then dehydrated in a series of ethanol baths and cleared in xylene overnight. The glands were stored in methyl salicylate until pictures were taken using a numeric camera (Sony Cybershot) or a SteREO Lumar V12 microscope (Zeiss).

Evaluation of ductal development

The distance of ductal migration was evaluated in virgin mice by measuring from the bottom of the lymph node to the end of the longest duct on the inguinal mammary gland using calipers. Ductal distance was recorded relative to the length of the mammary gland from the bottom of the lymph node to the edge of the fat pad in order to compensate for any mammary gland size differences between mutant and WT mice.

Haematoxylin and eosin staining

Mammary glands from Cx43^I130T/+ mice at parturition, lactation and involution were fixed in 10 % neutral-buffered formalin and embedded in paraffin. Paraffin-embedded sections (6 μm) were deparaffinized in xylene and rehydrated in descending concentrations of ethanol baths (100, 95, 70 and 50 %). Rehydrated tissues were stained in 1 % Harris's haematoxylin for 4 min followed by 1 % eosin for 2 min (Lerner Laboratories). Stained tissues were then rehydrated in ethanol baths (95 and 100 %) followed by xylene baths and mounted using Cytoseal (Richard-Allan Scientific). Images were captured using a 20× objective lens mounted on a Leica DM IRE2 inverted epifluorescence microscope equipped with a ProgRes C5 camera (Jenoptik) and ProgRes Mac CapturePro 2.7.6 imaging software.

Oxytocin-induced milk ejection assay

Pups were removed from the dam after feeding on parturition day. After 1 h, dams were killed and mammary glands were exposed as described previously [28]. PBS, or 8 pg/ml or 80 μg/ml oxytocin
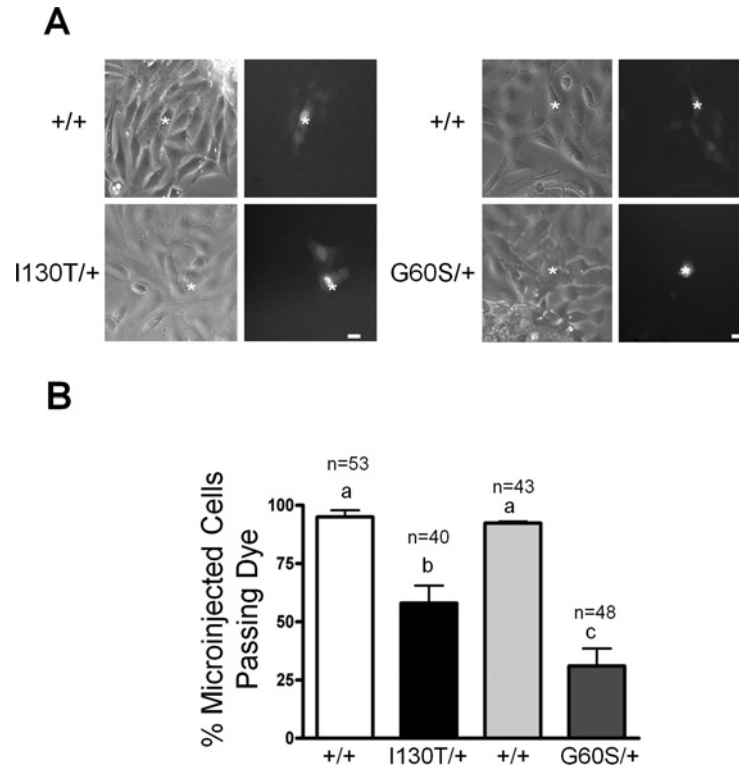
Figure 3   In comparison with controls, granulosa cells isolated from Cx43^I130T/+ mice are better coupled than cells from Cx43^G60S/+ mice

(**A**) Isolated granulosa cells were microinjected with Lucifer Yellow dye (asterisks). Scale bars = 10 μm. (**B**) Relative to controls, granulosa cells expressing the I130T mutant exhibited a higher incidence of dye coupling than those expressing the G60S mutant. Values are the mean percentage incidence of dye transfer $\pm$ S.E.M. from three experiments. *n* indicates the number of injections. Letters on top of columns represent statistical differences.

(Sigma) dissolved in PBS was applied directly to the mammary glands for 1 min and then removed. Milk entry into ducts was evaluated. Photographs were taken before and after exposure to PBS or oxytocin with a numeric camera (Sony Cybershot). Four mutant and WT littermate controls were used for this experiment.

Statistical analysis

Statistical analysis was performed using Student's unpaired *t* test or a one-way ANOVA test in which a $P < 0.05$ was considered significant. Values are presented as means $\pm$ S.E.M. All statistics were performed using GraphPad Prism version 4.03 for Windows.

RESULTS

The Cx43 I130T mutant has partial junctional conductance in gap-junction-deficient N2A cells

To determine whether the I130T and G60S Cx43 mutants had similar capacities to form functional gap junction channels, gap junctional communication-deficient N2A cells were engineered to individually express these mutants. Although N2A cells were observed to be free of functional gap junctional channels, cells expressing WT Cx43 were well coupled. Consistent with previous reports, cells expressing the I130T mutant showed a highly reduced *G*j compared with control Cx43-expressing cells, whereas the G60S mutant was found to be functionally dead (Figure 1) [17,23,29].

Primary myoepithelial and granulosa cells isolated from Cx43^I130T/+ mice are comparatively better coupled than cells from Cx43^G60S/+ mice

To determine whether primary mammary cells from Cx43^I130T/+ and Cx43^G60S/+ mice were differentially coupled in relation to their respective controls, cultured cells were microinjected with Lucifer Yellow and spread of the dye was assessed. On the basis of immunofluorescent labelling of keratin-14 and Cx43, mammary epithelium cultures were deemed highly enriched in myoepithelial cells and assembled gap junctions (Figure 2A). Similar to what we previously reported [27], dye transfer between myoepithelial cells isolated from Cx43^G60S/+ mice was severely reduced to ~39% of their WT control (Figures 2B and 2C). Interestingly, primary myoepithelial cell cultures from Cx43^I130T/+ mice showed a significant reduction in dye transfer, but coupling remained at ~71% of the WT control (Figures 2B and 2C). In addition, the incidence of dye spreading to two or more cells was significantly reduced to ~22% of controls in myoepithelial cells isolated from Cx43^G60S/+ mice, but was not significantly changed in myoepithelial cells isolated from Cx43^I130T/+ mice compared with the respective control (Figure 2D).

In support of the notion that the G60S mutant was a more potent inhibitor of dye transfer than the I130T mutant when normalized to their respective WT controls, granulosa cells of immature mouse ovarian follicles, which are known to only express Cx43, were isolated from mutant mice and assessed for dye transfer [30] (Figures 3A and 3B). Similar to our findings from myoepithelial cells, the incidence of dye transfer between granulosa cells of Cx43^I130T/+ mice was 61% of the control, whereas coupling in
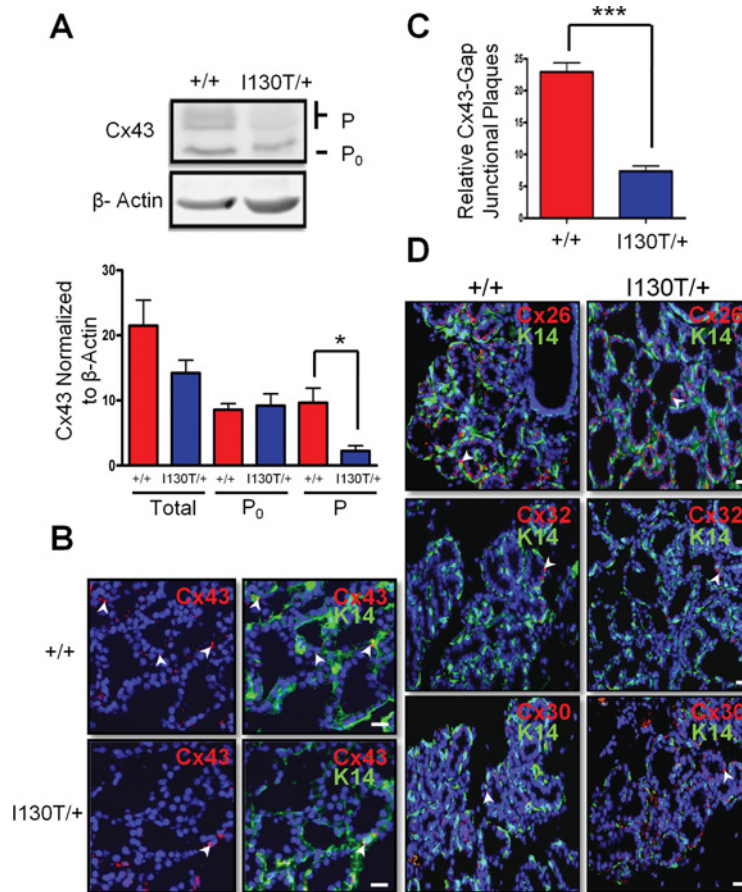
Figure 4   The highly phosphorylated species of Cx43 were reduced in the mammary gland of Cx43$^{I130T/+}$ mice at parturition, whereas co-expressed mammary gland connexins remain unchanged

(**A**) Western blot analysis of Cx43 revealed significantly reduced levels of the highly phosphorylated species (P) of Cx43, whereas the primarily unphosphorylated (P0) species remained similar to that found in littermate control mice. Values are mean levels of total, P0 and P relative to β-actin $\pm$ S.E.M. (*$P < 0.05$) ($n = 6$). (**B**) Mammary gland sections were immunolabelled for Cx43 (red) and keratin 14 (K14) (green), whereas nuclei were stained with Hoechst (blue). (**C**) Punctate Cx43 gap junction plaques (**B**, arrowheads) present at cell–cell interfaces of keratin-14-positive cells were significantly reduced in Cx43$^{I130T/+}$ mice compared with control mice (scale bars $= 20\ \mu$m). Values are the mean number of Cx43 gap junction plaques relative to the area of nuclei per 0.18 mm^2 $\pm$ S.E.M. (***$P < 0.001$; $n = 5$). (**D**) Paraffin-embedded mammary gland sections double-immunolabelled for Cx26, Cx32 or Cx30 (red), and keratin 14 (green) revealed a similar profile of gap junctions between mutant and control mice ($n = 6$).

Cx43$^{G60S/+}$ mouse granulosa cells was reduced to 33 % of the control. Collectively, the I130T mutant reduced GJIC to a lesser extent than the G60S mutant in primary cells known to express only Cx43.

### Highly phosphorylated species of Cx43 are reduced in the Cx43$^{I130T/+}$ mouse mammary gland

Western blot analysis of mammary glands from Cx43$^{I130T/+}$ mice at parturition revealed a non-significant decrease in total Cx43 compared with WT mice. However, as previously demonstrated in cardiac tissue [25], the highly phosphorylated species of Cx43 (P) was significantly reduced whereas the primarily unphosphorylated (P0) species of Cx43 remained unchanged in the Cx43$^{I130T/+}$ mutant mice (Figure 4A). Notably, the number of Cx43 gap junction plaques of mutant mice was significantly reduced compared with wild-type mice at parturition (Figures 4B and 4C). Consistent with previous reports, immunofluorescence revealed a similar distribution of Cx26, Cx32 and Cx30 gap junction plaques between luminal epithelial cells in Cx43$^{I130T/+}$ mice compared with controls (Figure 4D) [20,21]. Collectively,

the I130T mutant reduces the phosphorylation of total Cx43 and Cx43 gap junction plaques, with no obvious effect on other co-expressed mammary gland connexins.

Pre-pubertal Cx43$^{I130T/+}$ mice have smaller mammary glands with delayed ductal morphogenesis

To assess mammary gland development in virgin mice, both body and mammary gland weights were measured and compared between Cx43$^{I130T/+}$ and Cx43$^{+/+}$ mice. Body weights were similar between virgin Cx43$^{I130T/+}$ and Cx43$^{+/+}$ mice at all time points assessed (Figure 5A), yet mammary glands of 4 week Cx43$^{I130T/+}$ mice were significantly smaller than Cx43$^{+/+}$ mice (Figure 5B). However, no difference was observed in mutant mice following the onset of puberty at 7 and 10 weeks (Figure 5B). When corrected for body weights, relative mammary glands of pre-pubertal mice were significantly smaller than control mice, but there was no difference in relative gland weights after 7 weeks (Figure 5C).

In order to investigate the impact of the I130T Cx43 mutant on mammary gland development in virgin mice, mammary gland
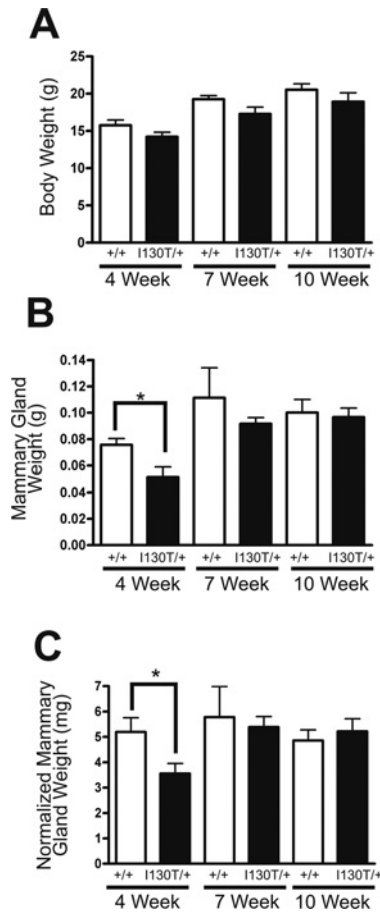
Figure 5   Pre-pubertal Cx43$^{I130T/+}$ mice have smaller mammary glands

(**A**) Body weights were recorded from virgin 4-, 7- and 10-week-old mice revealing similar body weights in Cx43$^{I130T/+}$ mice compared with littermate controls. Values are mean body weights $\pm$ S.E.M. (**B**) Inguinal mammary gland weights recorded in virgin mice revealed significantly reduced gland weight in mutant mice at 4 weeks. Values are the mean mammary gland weight $\pm$ S.E.M. (**C**) When normalized for body weight, mammary glands from 4-week-old mutant mice were significantly smaller compared with controls. Values are the mean normalized gland weight $\pm$ S.E.M. $*P < 0.05$ ($n = 6$).

architecture was evaluated through whole mounting. Consistent with normal mammary gland development, virgin Cx43$^{+/+}$ mice had numerous ducts with TEBs (terminal end buds) elongating within the stromal fat pad at 4 and 7 weeks, developing numerous side branches and filling the mammary fat pads by 10 weeks (Figures 6A–6C). At 4 weeks, Cx43$^{I130T/+}$ mice presented with many ducts having TEBs extending towards the lymph node within a well-developed stroma (Figure 6A); however, ductal length relative to the length of the gland was significantly delayed by ~ 45 % in mutant mice (Figure 6D). Interestingly, both 7- and 10-week-old mutant and control mice showed similar levels of ductal invasion, ductal lengths and side branches throughout the fat pad (Figures 6B–6D). Together, pre-pubertal Cx43$^{I130T/+}$ mice exhibit smaller mammary glands with delayed ductal development which was not observed following the onset of puberty.

Cx43$^{I130T/+}$ mice have smaller mammary glands at parturition and involution

To assess whether the I130T mutant affects the development of the mammary gland during pregnancy, lactation and involution,

body and mammary gland weight were evaluated in mutant and Cx43$^{+/+}$ mice. At parturition and lactation, body weight was similar in Cx43$^{I130T/+}$ mice compared with control mice (Figure 7A). However, body weight was significantly reduced by ~ 12 % in mutant mice compared with controls at involution (Figure 7A). Cx43$^{I130T/+}$ mice showed a significant reduction in mammary gland weight at parturition and involution and, when this was normalized to body weight, glands were ~ 20 % smaller at parturition and ~ 33 % smaller at involution compared with Cx43$^{+/+}$ mice (Figures 7B and 7C). Normalized mammary glands of mutant mice were similar to controls during lactation (Figure 7C). To assess whether changes in the weight of mutant and WT mice were the result of differences in prolactin hormone signalling, serum prolactin concentrations were assayed and found to be similar in Cx43$^{I130T/+}$ and Cx43$^{+/+}$ mice during mid-pregnancy (Figure 7D). Taken together, smaller mammary glands at parturition and involution suggests that gland developmental defects at these time points were not a result of reduced prolactin in the blood.

To identify whether the change in weight of mutant mouse mammary glands represented an acute indicator of structural changes within the gland, whole-mount analysis revealed mammary glands filled with alveoli and ducts from Cx43$^{I130T/+}$ mice at parturition and lactation, consistent with normal mammary gland development in control mice (Figure 8A). Following the onset of involution, mammary glands from Cx43$^{I130T/+}$ mice showed a reduction in the number of alveoli similar to Cx43$^{+/+}$ mice, suggesting that the epithelial compartment within the gland was in a similar stage of gland remodelling compared with the control (Figure 8A). Similarly, histological analysis revealed numerous alveoli and ducts with evidence of milk within the lumen of mutant and control mice at parturition and lactation (Figure 8B). In addition, mammary glands of both Cx43$^{I130T/+}$ and Cx43$^{+/+}$ mice had undergone extensive gland remodelling at involution, in which a reduction of alveoli was apparent within the stroma (Figure 8B).

In another assessment of potential changes in the mutant mouse mammary glands at parturition, paraffin-embedded mammary glands were immunolabelled with the proliferation marker PCNA. These studies revealed a significant decrease in the number of epithelial cells undergoing proliferation in Cx43$^{I130T/+}$ mice (Figure 9A). In addition, cleaved caspase 3 immunolabelling of mammary glands 48 h following weaning of pups showed minimal staining of cells undergoing apoptosis in Cx43$^{I130T/+}$ mice, similar to controls (Figure 9B). Collectively, dysregulation of proliferation in mammary glands at parturition, but not apoptotic mechanisms during involution, may account for changes in mammary gland weight in the Cx43$^{I130T/+}$ mice.

Cx43$^{I130T/+}$ mice show no signs of a lactational or milk-ejection defect

In order to assess whether the I130T mutant affected lactation in Cx43$^{I130T/+}$ mice, Western blot analysis of two commonly produced milk proteins, β-casein and WAP, revealed similar protein levels in mutant and control mice at parturition (Figures 10A and 10B). In addition, to assess whether Cx43$^{I130T/+}$ mice exhibited a defect in the contraction of myoepithelial cells, mammary glands of lactating mutant mice were assessed for milk entry into ducts following exposure to exogenous oxytocin. Similar to Cx43$^{+/+}$ mice, mutant mice showed the presence of low levels of milk within the ducts of the thoracic mammary glands prior to the addition of oxytocin (Figure 10C). Following treatment with 80 μg/ml or 8 pg/ml oxytocin, milk rapidly filled
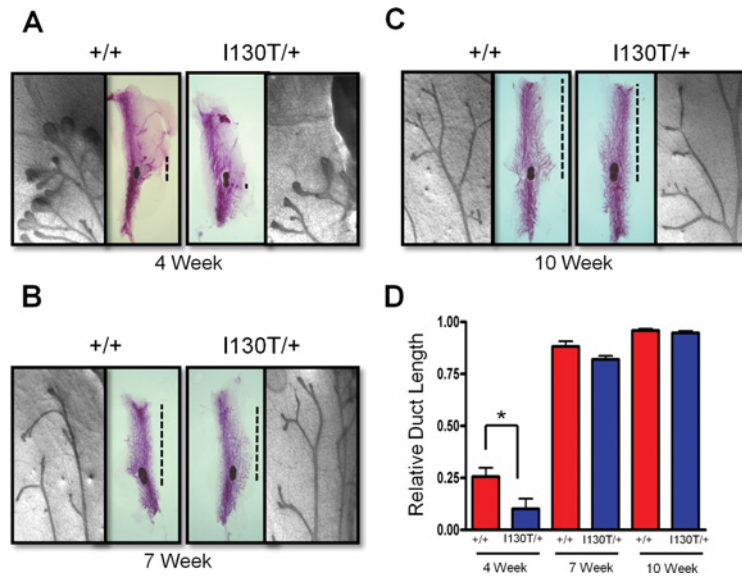
Figure 6   Pre-pubertal Cx43$^{I130T/+}$ mice have delayed mammary gland development

(A–C) Whole-mount analysis of 4, 7 and 10 week mutant and control mice revealed similar gland architecture with ducts elongating from TEBs through a developed stromal mammary fat pad. (D) Duct elongation from 4-week-old mutant mice was significantly delayed compared with controls. Values are the mean ductal extensions from the bottom of the lymph node to the furthest migrating duct (broken lines in A–C) relative to the length of the mammary gland from the bottom of the lymph node to the edge of the fat pad $\pm$ S.E.M. *$P < 0.05$ ($n = 6$).
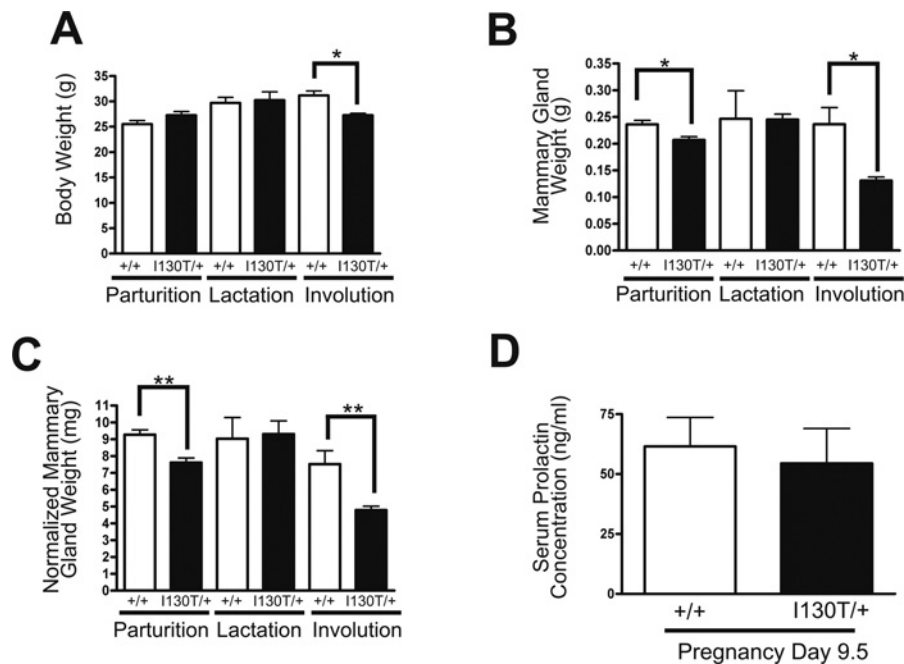
Figure 7   Cx43$^{I130T/+}$ mice have reduced mammary gland weights at parturition and involution

(A) Evaluation of body weights during parturition, lactation and involution revealed that Cx43$^{I130T/+}$ mice were significantly smaller compared with control mice at involution. Values are mean body weights $\pm$ S.E.M. ($n = 6$). (B and C) Mammary gland weight and normalized mammary gland weight were significantly reduced in Cx43$^{I130T/+}$ mice at parturition and involution compared with controls ($n = 6$). (D) Serum isolated from mutant and WT mice at mid-pregnancy contained similar levels of prolactin ($n = 4$). Values are means $\pm$ S.E.M. *$P < 0.05$; **$P < 0.01$.

the mammary gland ducts of Cx43$^{I130T/+}$ and control mice causing them to become easily observable (Figure 10D). These findings are consistent with the fact that Cx43$^{I130T/+}$ female mice can readily feed their pups. Together, mammary glands from mutant mice had no observable functional defects in milk production or ejection compared with control mice.

DISCUSSION

The focus of the present study was two aspects: first, to evaluate the critical role of Cx43 throughout all stages of mammary gland development with emphasis on the importance of Cx43-mediated GJIC; and second, to determine whether a Cx43 ODDD mutant

A

B
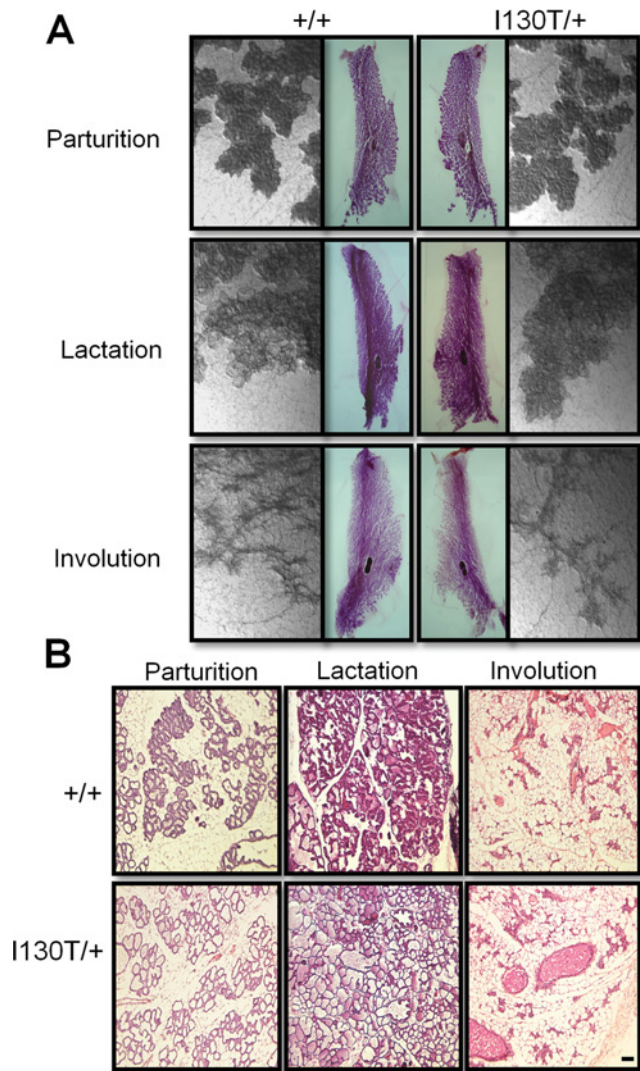
Figure 8   Lactating and involuting Cx43$^{I130T/+}$ mice have normal mammary gland architecture

(**A**) Whole-mount analysis of mice at parturition, lactation and involution revealed similar alveolar and ductal gland structure in mutant mice compared with controls. (**B**) Haematoxylin and eosin staining revealed similar histology in mutant and control mice at all time points. Scale bars = 100 μm. n = 6.

with residual channel-forming activity would be sufficient to prevent any functional or developmental defects in the mammary gland. In pursuit of these goals, we obtained a genetically modified mouse model of ODDD that harbours a germline autosomal-dominant I130T mutation. First, we determined that the Cx43 I130T mutant has partial channel activity when expressed in the absence of other connexins and does not appear to act as a dominant-negative, unlike the G60S mutant, when co-expressed with Cx43 in primary myoepithelial and granulosa cells. Secondly, we showed that, although they exhibited similar gland architecture, mammary glands from virgin pre-pubertal I130T mutant mice were smaller than matched controls and exhibited a delay in ductal elongation before the onset of puberty. Thirdly, we found that mammary glands from Cx43$^{I130T/+}$ mice were smaller than controls at parturition, due, in part, to impaired cell proliferation. Finally, we identified that mammary glands from I130T mutant mice exhibited no evidence of a defect in milk production or milk ejection. Thus we clearly demonstrated

that Cx43 is necessary for timely mammary gland development. In addition, we surmised that two distinct autosomal-dominant mutations in the *GJA1* gene encoding Cx43 (I130T and G60S) can manifest as distinctly different phenotypes during gland development that appear to be dependent on the potency of the mutation in inhibiting GJIC.

Differential coupling capacity of ODDD-linked mutants

ODDD mutants have previously been shown to present with differential abilities to traffic to cell–cell appositions and form plaques, to participate in GJIC and to act as dominant-negatives on the function of co-expressed WT Cx43 [23,29]. We evaluated the G60S and I130T mutants and found that only the I130T mutant retained partial junctional conductance when expressed alone in connexin-deficient N2A cells. This is consistent with previous studies [17,23,29] which also identified that the I130T mutant retained the ability to form gap junction plaques with residual coupling activity, whereas the G60S mutant was maintained mainly in an intracellular profile and functionally dead. However, in ODDD these individual mutants are always co-expressed with WT Cx43, thus their effect on total Cx43 function needed to be assessed in primary cells from mutant mice that express only Cx43. To that end, in both primary myoepithelial and granulosa cells we discovered that the I130T mutant caused a smaller reduction in dye transfer compared with the G60S mutant when normalized to their appropriate control counterparts. Consistently, we and others [17,25] have reported a more severe loss of GJIC in primary cells from G60S mutant mice, but the results of the present study are the first to directly compare these two mutants in parallel experiments. Thus we hypothesized that a higher basal level of total Cx43 function in I130T mutant mice might retain a more normal mammary gland function than we previously documented in the G60S mutant mice where the gland exhibits significant developmental delays and failed to eject milk [20].

Cx43 is known to be expressed in the mammary gland throughout development and differentiation, and evidence suggests that, at parturition, Cx43 levels increase and the more highly phosphorylated species of Cx43 become more evident [14]. Similar to our findings in myoepithelial and granulosa cells, Kalcheva et al. [25] showed that the highly phosphorylated species of Cx43 were less prevalent in cardiomyocytes of I130T mutant mice and this was accompanied by a reduction in Cx43 gap junctional plaques. Thus the reduction in GJIC observed in cells isolated from I130T mutant mice was not surprising as the highly phosphorylated species of Cx43 have been correlated with the level of Cx43 assembled into functional gap junction plaques [31]. Not unlike our observations in the Cx43$^{G60S/+}$ mice [20,21], changes in Cx43 expression and phosphorylation had no effects on Cx26, Cx30 or Cx32, suggesting no cross-talk between Cx43 changes and other mammary gland connexins.

A full complement of Cx43 is necessary for the regulated development of mammary glands in virgin mice

Before puberty, ductal elongation is largely hormone-independent and is believed to be regulated by locally acting factors between the epithelium and the stroma [6,32]. At 4 weeks, Cx43$^{G60S/+}$ mice exhibited a delay in ductal elongation and severely impaired stromal development, suggesting a role for Cx43 in ductal morphogenesis before puberty [20]. Although it is unknown if the delay in ductal development is a result of dysregulation of Cx43 in the stroma or in the epithelium, extracellular matrix components are able to bind and sequester signalling molecules that affect ductal/branching morphogenesis,
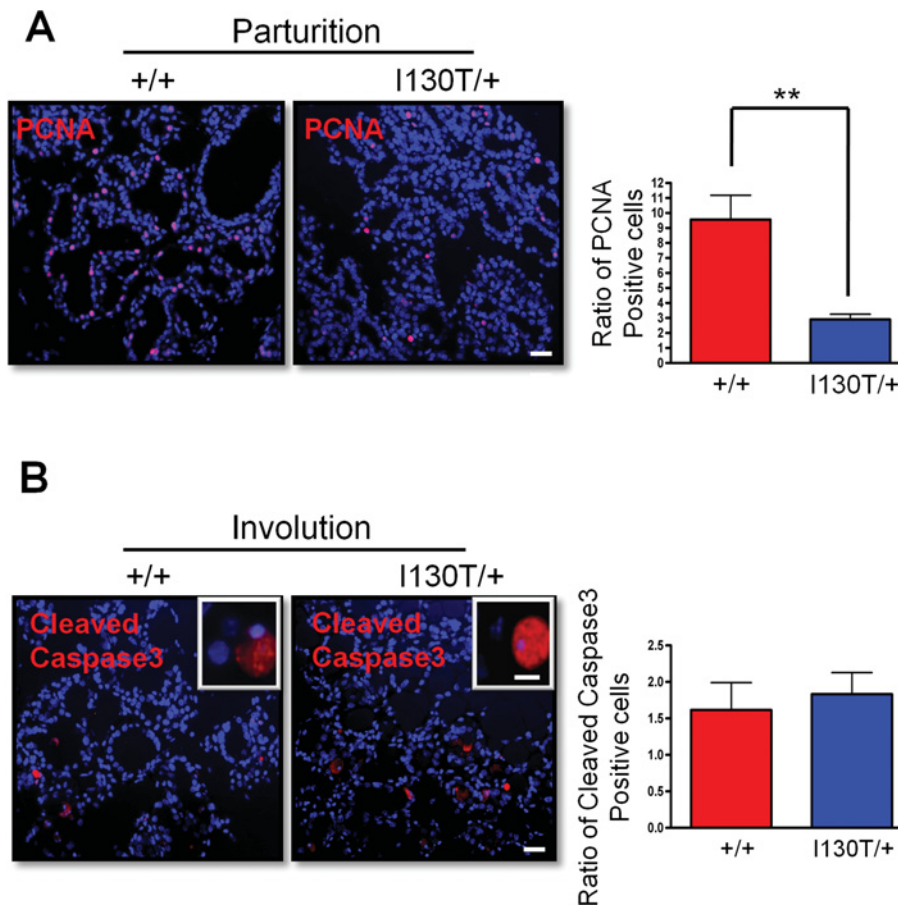
Figure 9   Mammary glands from Cx43$^{I130T/+}$ mice exhibited a reduction in proliferation at parturition

(**A**) Assessment of the proliferation marker PCNA in paraffin-embedded mammary glands at parturition revealed a significant decrease in cell proliferation in Cx43$^{I130T/+}$ mice compared with controls (**$P < 0.01$). (**B**) Evaluation of the apoptotic marker cleaved caspase 3 at involution revealed no change between mutant and control mice. Values are mean positive cells relative to the area of nuclei per 0.18 mm^2 $\pm$ S.E.M. Scale bars $= 50$ μm (10 μm for inserts). $n = 6$.

suggesting that improper stromal development may contribute to the delay in ductal elongation observed in Cx43$^{G60S/+}$ mice [33]. Interestingly, although slightly smaller mammary glands were observed in Cx43$^{I130T/+}$ mice at 4 weeks, these mice displayed a delay in ductal differentiation despite exhibiting relatively normal stromal development, suggesting that the poorly developed stroma in Cx43$^{G60S/+}$ mice was not the only contributing factor underlying the delay in development. As such, our evidence provides support for a role of epithelium-localized Cx43 in regulating ductal growth prior to the onset of puberty.

At puberty, ductal growth becomes oestrogen-dependent which is exemplified by the fact that oestrogen receptor α-knockout mice have limited ductal elongation during puberty [34]. In Cx43$^{G60S/+}$ mice, the onset of hormones at puberty was unable to overcome the delay in development observed in pre-pubertal mice, even after 10 weeks. Thus we suggested that GJIC may in part mediate oestrogen signalling between the epithelium and stroma [20]. Interestingly, ductal length from Cx43$^{I130T/+}$ mice was similar to WT mice 1 week following the onset of puberty, suggesting three possible roles for Cx43 in pubertal ductal morphogenesis. First, that oestrogen-driven signalling of ductal morphogenesis may not be dependent on GJIC and that the delay in development observed in Cx43$^{G60S/+}$ following puberty was a result of improper stromal development [20]. Secondly, that the delay in ductal morphogenesis following puberty is a result of GJIC-independent mechanisms, which are further dependent on the mutant

expressed. This concept is supported by the observation that Wnt5a-overexpressing mice, in which Wnt5a overexpression was shown to decrease GJIC *in vitro*, had similar ductal morphogenesis compared with controls [35]. However, whether GJIC is reduced in the virgin mammary gland of Wnt5a-overexpressing mice is unknown, thus limiting the impact of these results. Thirdly, the higher residual Cx43 function observed in mammary cells of Cx43$^{I130T/+}$ mice, that is nearly double that seen in Cx43$^{G60S/+}$ mice, is sufficient to mediate oestrogen or other hormonal signals during ductal morphogenesis. Although further mechanistic details remain to be elucidated, it is clear that Cx43 plays a role in regulating the development of the mammary gland in virgin mice.

Cx43 regulates proliferation in the mammary gland following the onset of pregnancy

Following the onset of pregnancy, the mammary gland enlarges as the epithelial to adipocyte ratio increases as a result of extensive proliferation [5]. Similar to what we have reported for the Cx43$^{G60S/+}$ mice [20], mammary glands of Cx43$^{I130T/+}$ mice were significantly smaller at parturition compared with WT controls, but in the present study we extend our understanding of the process by showing that the defect was due to reduced cell proliferation in Cx43$^{I130T/+}$ mice. Cx43 has previously been implicated in pathways that affect regulators of the cell cycle such as cyclin D1 [36]. Interestingly, cyclin D1-null mice have poor
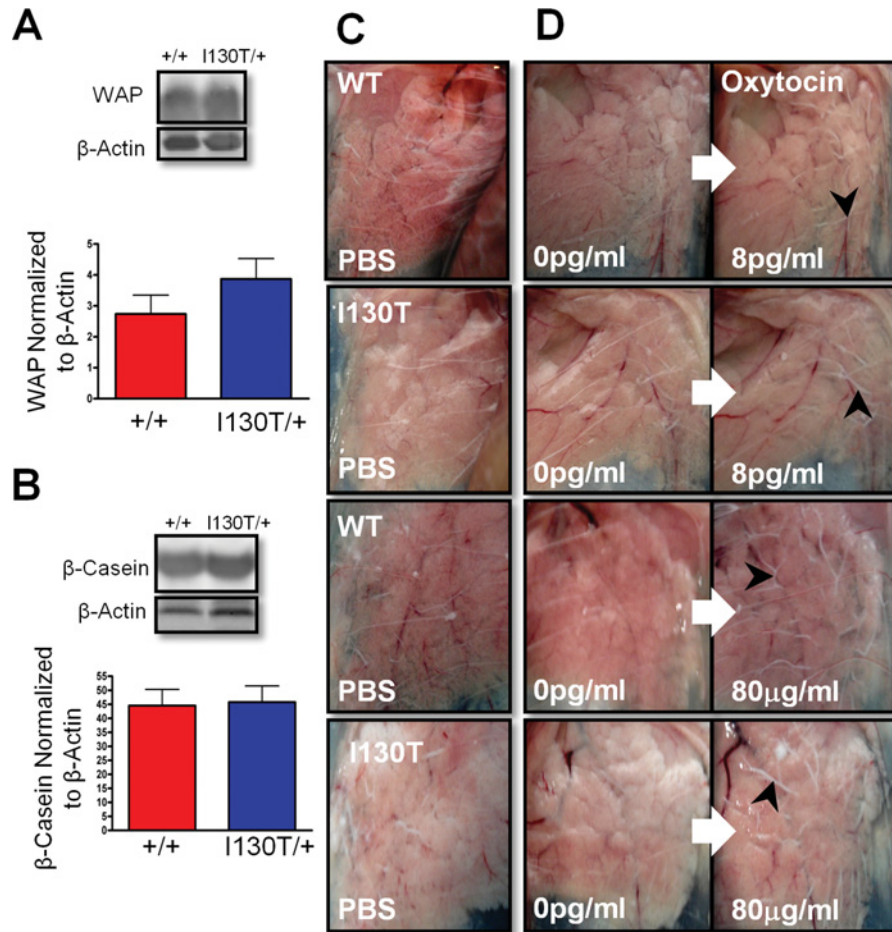
Figure 10   Lactating Cx43$^{I130T/+}$ mice can produce and eject milk into ducts upon oxytocin stimulation

(**A** and **B**) Western blot analysis revealed that Cx43$^{I130T/+}$ mice express the common milk proteins WAP and β-casein, similar to controls. Values are mean expression $\pm$ S.E.M. (**C** and **D**). An oxytocin-induced milk-ejection assay revealed that lactating Cx43$^{I130T/+}$ mice respond to exogenous oxytocin to deliver milk into ducts (arrowheads). Images in (**D**) represent the same gland field before and after (separated by arrows) the addition of oxytocin. $n = 4$.

alveolar development during pregnancy as a result of reduced proliferation, suggesting a possible regulatory pathway between Cx43 and cyclin D1 [37]. It is also important to note that both ODDD mutant mouse models showed similar gland architecture and histology suggesting that the role of Cx43 in proliferation of the mammary gland is not critical for development of the gland during pregnancy.

After weaning of the pups, the mammary gland undergoes involution, which is characterized by both apoptotic cell death of epithelial cells and stromal activation [38]. Compared with their control counterparts, Cx43$^{I130T/+}$ mice had significantly smaller mammary glands 2 days post-weaning suggesting accelerated involution, but this was not supported by the gross and histological evaluation of the epithelial ducts which revealed no observable difference. In addition, the level of apoptosis within the glands was similar to the control. Therefore the decrease in mammary gland weight observed in Cx43$^{I130T/+}$ mice probably reflects changes in the stromal compartment of the gland, which is composed mainly of adipocytes. Importantly, the gap junction blocker 18-α-glycyrrhetinic acid and siRNA (small interfering RNA) knockdown of Cx43 have previously been shown to inhibit adipogenesis in pre-adipocytes, suggesting a role for Cx43 in regulating adipocyte differentiation [39].

Given the systemic reduction in Cx43 function in I130T mutant mice and the fact that this genetic modification causes a small reduction in the body weight of mutant mice, it is possible that hormonal signalling which regulates mammary gland development is altered due to the compromised role of Cx43 in endocrine glands, such as the ovaries, adrenal gland or pituitary gland [40]. To investigate this, we hypothesized that changes in Cx43 affected prolactin regulation which is supported by correlational evidence that an increase in Cx43 is associated with an increase in prolactin secretion [41]. Furthermore, prolactin receptor-knockout mice exhibit reduced adipose tissue weight throughout the body, including the mammary gland, as a result of decreased adipocyte cell numbers, suggesting a role for prolactin in adipocyte proliferation and differentiation [42]. Our evaluation of serum prolactin levels at mid-pregnancy revealed no significant differences in mutant and WT mice, suggesting that reduced Cx43 function does not affect secretion of prolactin into the blood. However, it is unknown whether changes in Cx43 alter prolactin signalling downstream in the mammary glands at the level of the prolactin receptor or whether this reflects changes in other hormones. Thus we conclude that loss-of-function mutations in Cx43 may directly or indirectly affect the stromal component of the mammary gland during involution.

Partial coupling by Cx43 gap junction channels is sufficient for normal mammary gland function

Together with our previous findings using Cx43$^{G60S/+}$ mutant mice [21], the results of the present study strongly support the conclusion that a full complement of Cx43 is not necessary for the synthesis of constitutive proteins of milk. Owing to Cx43 being mainly restricted to myoepithelial cells of mammary gland epithelium, previous studies have suggested that Cx43 plays a role in myoepithelial differentiation, co-ordinated myoepithelial contraction and proper milk ejection [7,14]. However, it was not until our evaluation of Cx43$^{G60S/+}$ mice at parturition that we determined that Cx43 was essential for proper oxytocin-induced milk ejection. This finding was later supported following examination of Wnt-5a-overexpressing mice that presented with a similar ejection defect which the authors linked to severely impaired Cx43-mediated GJIC [35]. Surprisingly, Cx43$^{I130T/+}$ mice exhibited no apparent defect in milk ejection upon oxytocin stimulation and females could readily feed pups. Given that myoepithelial cells from Cx43$^{I130T/+}$ mice are approximately twice as well coupled by Cx43 gap junctions as cells from the Cx43$^{G60S/+}$ mice, we conclude that there was sufficient residual Cx43-based GJIC to rescue the milk-ejection defect. This idea that different mutants of ODDD result in differential changes in the molecular properties of the Cx43 gap junctional channel has been suggested to contribute, in part, to the pleiotropic phenotype observed in ODDD patients [19]. However, it is also important to note that differences observed in myoepithelial GJIC may be due, in part, to the different mixed mouse strain backgrounds being studied, although both mutant mouse lines have been partially backcrossed to BL6. Importantly, the ODDD patient population includes all ethnic groups of mixed origin, suggesting that the variations observed in the mutant mice being studied may in fact best reflect the heterogeneity of the disease in the human patient population.

In summary, unlike the previously studied Cx43$^{G60S/+}$ mice with severely compromised Cx43 function, we found that Cx43$^{I130T/+}$ mice with partial Cx43 mutant channel function present with limited mammary gland developmental defects. In essence, severe defects in mammary gland function appear to require in excess of a 50 % reduction in total Cx43 function, which is consistent with the fact that Cx43$^{+/-}$ heterozygous knockout mice, expressing only a 50 % complement of Cx43, are relatively normal and have no evidence of lactation or milk-ejection defects [43]. In conclusion, we predict that ODDD patients which harbour mutations that maintain total Cx43 function in the breast at 50 % or better will not suffer from milk production or ejection defects, as appears to be the case for the vast majority of documented ODDD patients to date. Importantly, the present study also highlights the fact that the use of multiple genetically-modified mouse models is beneficial for establishing results that translate to different populations of ODDD patients.

AUTHOR CONTRIBUTION

Michael Stewart designed and performed experiments, interpreted the results, wrote the paper, and was involved in breeding the mice. Kevin Barr assisted in mouse breeding and isolated the primary granulosa cells. Xiang-Qun Gong performed the patch-clamp recording experiments under the supervision of Donglin Bai. Glenn Fishman engineered the Cx43$^{I130T/+}$ mice and provided these mice to the Laird laboratory. Dale Laird is the principal investigator and provided support throughout the study.

ACKNOWLEDGMENTS

We thank Dr Isabelle Plante, Dr Silvia Penuela and Dr Qing Shao for helpful advice and technical troubleshooting. We would also like to thank Shreya Podder for providing experimental assistance. We would like to thank Dr Janet Rossant at the Centre for Modeling Human Disease (Toronto, ON, Canada) for providing the Cx43$^{G60S/+}$ mice.

REFERENCES

1 Paznekas, W. A., Boyadjiev, S. A., Shapiro, R. E., Daniels, O., Wollnik, B., Keegan, C. E., Innis, J. W., Dinulos, M. B., Christian, C., Hannibal, M. C. and Jabs, E. W. (2003) Connexin 43 (GJA1) mutations cause the pleiotropic phenotype of oculodentodigital dysplasia. Am. J. Hum. Genet. **72**, 408–418

2 Laird, D. W. (2006) Life cycle of connexins in health and disease. Biochem. J. **394**, 527–543

3 El-Saghir, J. A., El-Habre, E. T., El-Sabban, M. E. and Talhouk, R. S. (2011) Connexins: a junctional crossroad to breast cancer. Int. J. Dev. Biol. **55**, 773–780

4 Hennighausen, L. and Robinson, G. W. (2005) Information networks in the mammary gland. Nat. Rev. Mol. Cell Biol. **6**, 715–725

5 Lamote, I., Meyer, E., Massart-Leen, A. M. and Burvenich, C. (2004) Sex steroids and growth factors in the regulation of mammary gland proliferation, differentiation, and involution. Steroids **69**, 145–159

6 Howlin, J., McBryan, J. and Martin, F. (2006) Pubertal mammary gland development: insights from mouse models. J. Mammary Gland Biol. Neoplasia **11**, 283–297

7 McLachlan, E., Shao, Q. and Laird, D. W. (2007) Connexins and gap junctions in mammary gland development and breast cancer progression. J. Membr. Biol. **218**, 107–121

8 Monaghan, P., Clarke, C., Perusinghe, N. P., Moss, D. W., Chen, X. Y. and Evans, W. H. (1996) Gap junction distribution and connexin expression in human breast. Exp. Cell Res. **223**, 29–38

9 Tomasetto, C., Neveu, M. J., Daley, J., Horan, P. K. and Sager, R. (1993) Specificity of gap junction communication among human mammary cells and connexin transfectants in culture. J. Cell Biol. **122**, 157–167

10 Locke, D., Stein, T., Davies, C., Morris, J., Harris, A. L., Evans, W. H., Monaghan, P. and Gusterson, B. (2004) Altered permeability and modulatory character of connexin channels during mammary gland development. Exp. Cell Res. **298**, 643–660

11 Locke, D., Jamieson, S., Stein, T., Liu, J., Hodgins, M. B., Harris, A. L. and Gusterson, B. (2007) Nature of Cx30-containing channels in the adult mouse mammary gland. Cell Tissue Res. **328**, 97–107

12 El-Sabban, M. E., Abi-Mosleh, L. F. and Talhouk, R. S. (2003) Developmental regulation of gap junctions and their role in mammary epithelial cell differentiation. J. Mammary Gland Biol. Neoplasia **8**, 463–473

13 Talhouk, R. S., Elble, R. C., Bassam, R., Daher, M., Sfeir, A., Mosleh, L. A., El-Khoury, H., Hamoui, S., Pauli, B. U. and El-Sabban, M. E. (2005) Developmental expression patterns and regulation of connexins in the mouse mammary gland: Expression of connexin30 in lactogenesis. Cell Tissue Res. **319**, 49–59

14 Yamanaka, I., Kuraoka, A., Inai, T., Ishibashi, T. and Shibata, Y. (1997) Changes in the phosphorylation states of connexin43 in myoepithelial cells of lactating rat mammary glands. Eur. J. Cell Biol. **72**, 166–173

15 Gudjonsson, T., Ronnov-Jessen, L., Villadsen, R., Rank, F., Bissell, M. J. and Petersen, O. W. (2002) Normal and tumor-derived myoepithelial cells differ in their ability to interact with luminal breast epithelial cells for polarity and basement membrane deposition. J. Cell Sci. **115**, 39–50

16 Adriance, M. C., Inman, J. L., Petersen, O. W. and Bissell, M. J. (2005) Myoepithelial cells: good fences make good neighbors. Breast Cancer Res. **7**, 190–197

17 Flenniken, A. M., Osborne, L. R., Anderson, N., Ciliberti, N., Fleming, C., Gittens, J. E., Gong, X. Q., Kelsey, L. B., Lounsbury, C., Moreno, L. et al. (2005) A Gja1 missense mutation in a mouse model of oculodentodigital dysplasia. Development **132**, 4375–4386

18 Toth, K., Shao, Q., Lorentz, R. and Laird, D. W. (2010) Decreased levels of Cx43 gap junctions result in ameloblast dysregulation and enamel hypoplasia in Gja1$^{Jrt/+}$ mice. J. Cell. Physiol. **223**, 601–609

19 Paznekas, W. A., Karczeski, B., Vermeer, S., Lowry, R. B., Delatycki, M., Laurence, F., Koivisto, P. A., Van Maldergem, L., Boyadjiev, S. A. et al. (2009) GJA1 mutations, variants, and connexin 43 dysfunction as it relates to the oculodentodigital dysplasia phenotype. Hum. Mutat. **30**, 724–733

20 Plante, I. and Laird, D. W. (2008) Decreased levels of connexin43 result in impaired development of the mammary gland in a mouse model of oculodentodigital dysplasia. Dev. Biol. **318**, 312–322

21 Plante, I., Wallis, A., Shao, Q. and Laird, D. W. (2010) Milk secretion and ejection are impaired in the mammary gland of mice harboring a Cx43 mutant while expression and localization of tight and adherens junction proteins remain unchanged. Biol. Reprod. **82**, 837–847

22 Amador, C., Mathews, A. M., Del Carmen Montoya, M., Laughridge, M. E., Everman, D. B. and Holden, K. R. (2008) Expanding the neurologic phenotype of oculodentodigital dysplasia in a 4-generation hispanic family. J. Child Neurol. **23**, 901–905

23 Seki, A., Coombs, W., Taffet, S. M. and Delmar, M. (2004) Loss of electrical communication, but not plaque formation, after mutations in the cytoplasmic loop of connexin43. Heart Rhythm. **1**, 227–233

24 Wasseff, S., Abrams, C. K. and Scherer, S. S. (2010) A dominant connexin43 mutant does not have dominant effects on gap junction coupling in astrocytes. Neuron Glia Biol. **6**, 213–223

25 Kalcheva, N., Qu, J., Sandeep, N., Garcia, L., Zhang, J., Wang, Z., Lampe, P. D., Suadicani, S. O., Spray, D. C. and Fishman, G. I. (2007) Gap junction remodeling and cardiac arrhythmogenesis in a murine model of oculodentodigital dysplasia. Proc. Natl. Acad. Sci. U.S.A. **104**, 20512–20516

26 Gong, X. Q., Shao, Q., Langlois, S., Bai, D. and Laird, D. W. (2007) Differential potency of dominant negative connexin43 mutants in oculodentodigital dysplasia. J. Biol. Chem. **282**, 19190–19202

27 Plante, I. and Laird, D. W. (2008) Decreased levels of connexin43 result in impaired development of the mammary gland in a mouse model of oculodentodigital dysplasia. Dev. Biol. **318**, 312–322

28 Plante, I., Stewart, M. K. and Laird, D. W. (2011) Evaluation of mammary gland development and function in mouse models. J. Vis. Exp. **53**, 2828

29 Shibayama, J., Paznekas, W., Seki, A., Taffet, S., Jabs, E. W., Delmar, M. and Musa, H. (2005) Functional characterization of connexin43 mutations found in patients with oculodentodigital dysplasia. Circ. Res. **96**, e83–e91

30 Kidder, G. M. and Mhawi, A. A. (2002) Gap junctions and ovarian folliculogenesis. Reproduction **123**, 613–620

31 Solan, J. L. and Lampe, P. D. (2009) Connexin43 phosphorylation: structural changes and biological effects. Biochem. J. **419**, 261–272

32 Howlett, A. R. and Bissell, M. J. (1993) The influence of tissue microenvironment (stroma and extracellular matrix) on the development and function of mammary epithelium. Epithelial Cell Biol. **2**, 79–89

33 Silberstein, G. B., Flanders, K. C., Roberts, A. B. and Daniel, C. W. (1992) Regulation of mammary morphogenesis: evidence for extracellular matrix-mediated inhibition of ductal budding by transforming growth factor-β1. Dev. Biol. **152**, 354–362

34 Bocchinfuso, W. P. and Korach, K. S. (1997) Mammary gland development and tumorigenesis in estrogen receptor knockout mice. J. Mammary Gland Biol. Neoplasia **2**, 323–334

35 Baxley, S. E., Jiang, W. and Serra, R. (2011) Misexpression of wingless-related MMTV integration site 5A in mouse mammary gland inhibits the milk ejection response and regulates connexin43 phosphorylation. Biol. Reprod. **85**, 907–915

36 Chen, S. C., Pelletier, D. B., Ao, P. and Boynton, A. L. (1995) Connexin43 reverses the phenotype of transformed cells and alters their expression of cyclin/cyclin-dependent kinases. Cell Growth Differ. **6**, 681–690

37 Fantl, V., Stamp, G., Andrews, A., Rosewell, I. and Dickson, C. (1995) Mice lacking cyclin D1 are small and show defects in eye and mammary gland development. Genes Dev. **9**, 2364–2372

38 O'Brien, J., Martinson, H., Durand-Rougely, C. and Schedin, P. (2012) Macrophages are crucial for epithelial cell death and adipocyte repopulation during mammary gland involution. Development **139**, 269–275

39 Yanagiya, T., Tanabe, A. and Hotta, K. (2007) Gap-junctional communication is required for mitotic clonal expansion during adipogenesis. Obesity **15**, 572–582

40 Serre-Beinier, V., Mas, C., Calabrese, A., Caton, D., Bauquis, J., Caille, D., Charollais, A., Cirulli, V. and Meda, P. (2002) Connexins and secretion. Biol. Cell **94**, 477–492

41 Vitale, M. L., Cardin, J., Gilula, N. B., Carbajal, M. E. and Pelletier, R. M. (2001) Dynamics of connexin 43 levels and distribution in the mink (M*ustela vison*) anterior pituitary are associated with seasonal changes in anterior pituitary prolactin content. Biol. Reprod. **64**, 625–633

42 Ormandy, C. J., Binart, N. and Kelly, P. A. (1997) Mammary gland development in prolactin receptor knockout mice. J. Mammary Gland Biol. Neoplasia **2**, 355–364

43 Reaume, A. G., de Sousa, P. A., Kulkarni, S., Langille, B. L., Zhu, D., Davies, T. C., Juneja, S. C., Kidder, G. M. and Rossant, J. (1995) Cardiac malformation in neonatal mice lacking connexin43. Science **267**, 1831–1834